Supporting Information

Embedding of superparamagnetic iron oxide nanoparticles into membranes of well-defined poly(ethylene oxide)-*block*-poly(ε-caprolactone) nanovesicles as ultrasensitive MRI probes of membrane bio-degradation

Adeline Hannecart,[a] Dimitri Stanicki,[a] Luce Vander Elst,[a] Robert N. Muller,[a,b] Annie Brûlet[c], Olivier Sandre,[d] Christophe Schatz,[d] Sébastien Lecommandoux[d] and Sophie Laurent*[a,b]

[a]Department of General, Organic and Biomedical Chemistry, NMR and Molecular Imaging Laboratory, University of Mons, 19 avenue Maistriau B-7000 Mons, Belgium

[b]Center for Microscopy and Molecular Imaging, 8 rue Adrienne Bolland, B-6041 Charleroi, Belgium

[c]Laboratoire Léon Brillouin, UMR12 CNRS / CEA Saclay, 91191 Gif sur Yvette, France

[d]Laboratoire de Chimie des Polymères Organiques, UMR5629 CNRS / Université de Bordeaux, ENSCBP 16 avenue Pey Berland F-33607 Pessac, France

Determination of the composition of PEO-*b*-PCL copolymer by ^{1}H NMR

^{1}H NMR spectrum of PEO-*b*-PCL copolymer was recorded at 500 MHz in $CDCl_3$ (Fig. S1).

The peak at 3.65 ppm is attributed to the methylene protons of the ethylene oxide units of PEO (protons B + B'). The peak corresponding to two protons of the last EO unit connected to PCL block (protons C) is lost in the background noise. As the average number of EO units is 45 (the synthesis was performed with PEO possessing an average molecular weight of 2000 g/mol), the integral intensity of the signal at 3.65 ppm (protons B and B') was set to 178.

Methylene protons of the **ε**-caprolactone units of PCL segment appeared as four signals at 4.07 ppm, 2.32 ppm, 1.65 ppm and 1.40 ppm as marked in figure S1. A degree of polymerization of PCL block (DP_{CL}) equal to 111 was determined from the integral intensity of the well-resolved peak at 4.07 ppm ($I_{4.07\ ppm}$) according to the equation S.1. The peak corresponding to two protons of the last CL unit connected to the hydroxyl group (protons H) is lost in the background noise.

$$DP_{CL} = (I_{4.07\ ppm} + 2) / 2 \qquad (S.1)$$

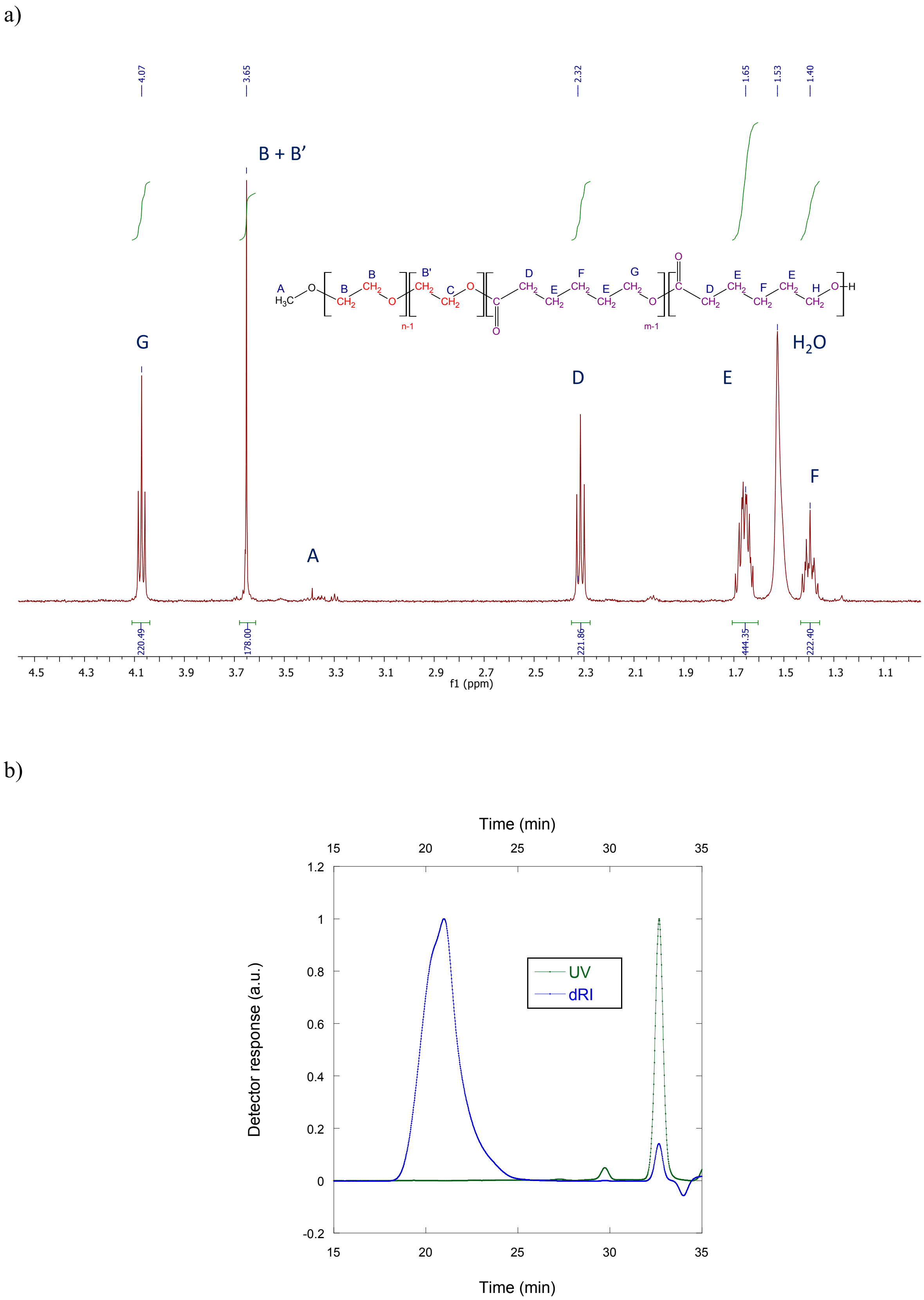

Figure S1. (a) 500 MHz ^{1}H NMR spectrum of PEO_{45}-*b*-PCL_{111} copolymer in $CDCl_3$; (b) GPC chromatogram of PEO_{45}-*b*-PCL_{111} obtained in THF (only UV and RI detector signals are plotted, the flow marker peak at 32.6 min being ascribed to 1,2,4-trichlorobenzene added in the eluent). The copolymer molar mass dispersity deduced is $Đ=M_w/M_n=1.35$.

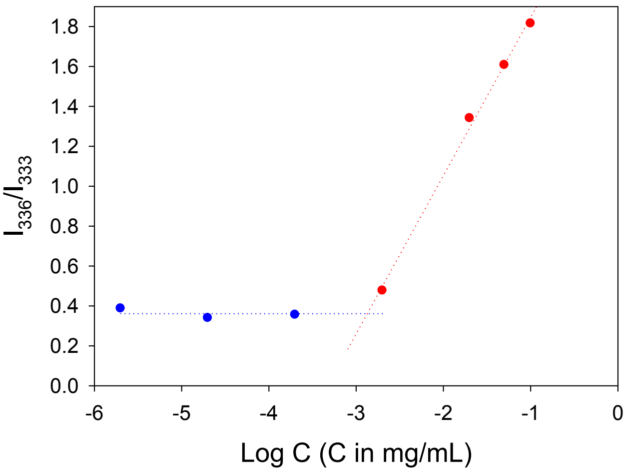

Figure S2. Plot of the I_{336}/I_{331} ratio against the logarithm of concentration of PEO_{45}-*b*-PCL_{111} suspensions in the presence of pyrene at fixed concentration of 0.6 µM.

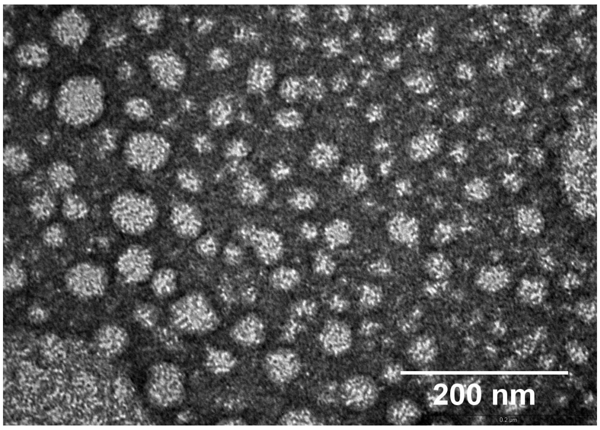

Figure S3. TEM images of PEO_{45}-*b*–PCL_{111} polymersomes negatively stained with uranyl acetate (scale bar = 200 nm)

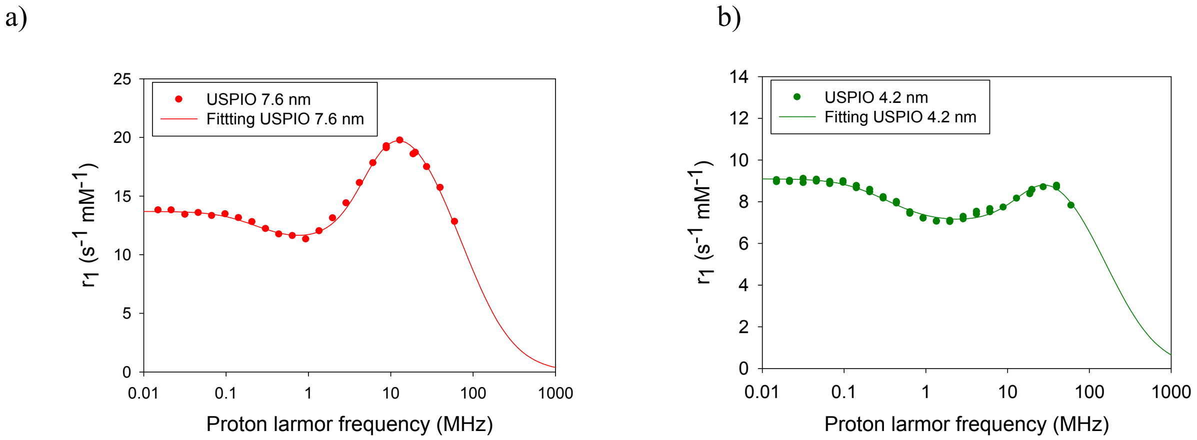

Figure S4. NMRD profiles of the longitudinal relaxivity *vs.* proton Larmor resonance frequency at 37°C for (a) 7.6 nm and (b) 4.2 nm USPIOs in THF. The fitting parameters are given in Table 1.

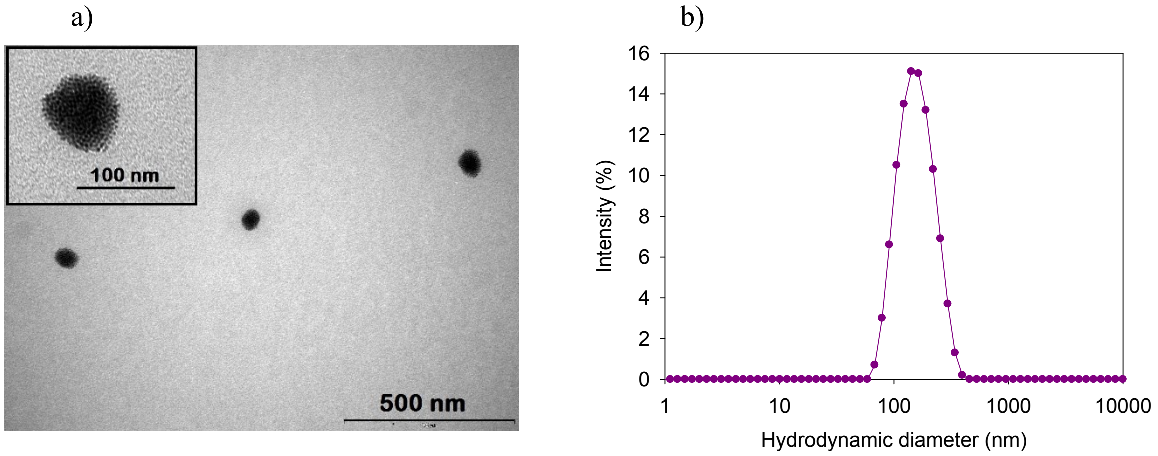

Figure S5. Size and morphology of PEO$_{45}$-*b*-PCL$_{111}$ vesicles loaded at 32% FWR with iron oxide nanoparticles of 4.2 nm diameter. (a) Low magnification TEM image showing vesicles with a high payload of USPIO (scale bar = 500 nm). The inset shows a close-up view of one vesicle (scale bar = 100 nm). (b) Intensity-weighted size distribution measured by DLS (D_H = 146 nm, PDI^{DLS} = 0.10).

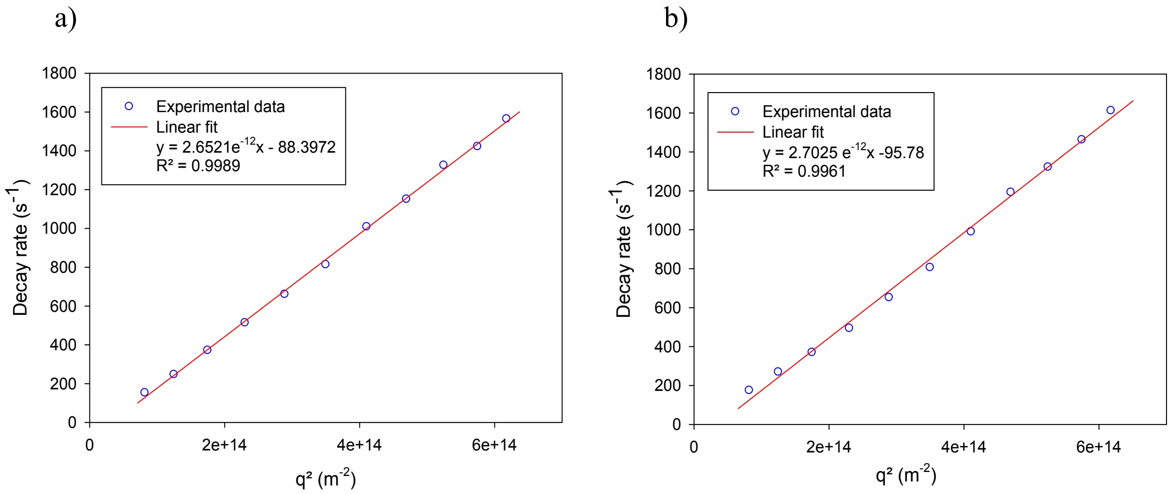

Figure S6. Multi-angle DLS plots: Variations of decay rate *Γ versus* squared scattering vector q^2 measured by multi-angle DLS by applying a CONTIN fit on a) Nanoprecipitated objects made by co-assembly of PEO$_{45}$-*b*-PCL$_{111}$ with 7.6 nm USPIO at 16% FWR and at a concentration of 0.11 mg·mL^{-1}

and b) Nanoprecipitated objects by co-assembly of PEO$_{45}$-*b*-PCL$_{111}$ with 4.2 nm USPIO at 32% FWR and at a concentration of 0.052 mg·mL^{-1}. The slopes lead to the diffusion constants of the objects, respectively 2.65 10^{-12} m²/s^{-1} (a) and 2.70 10^{-12} m²/s^{-1} (b), from which the hydrodynamic radii are calculated using Stokes-Einstein's equation, respectively 92.0 nm (a) and 90.3 nm (b).

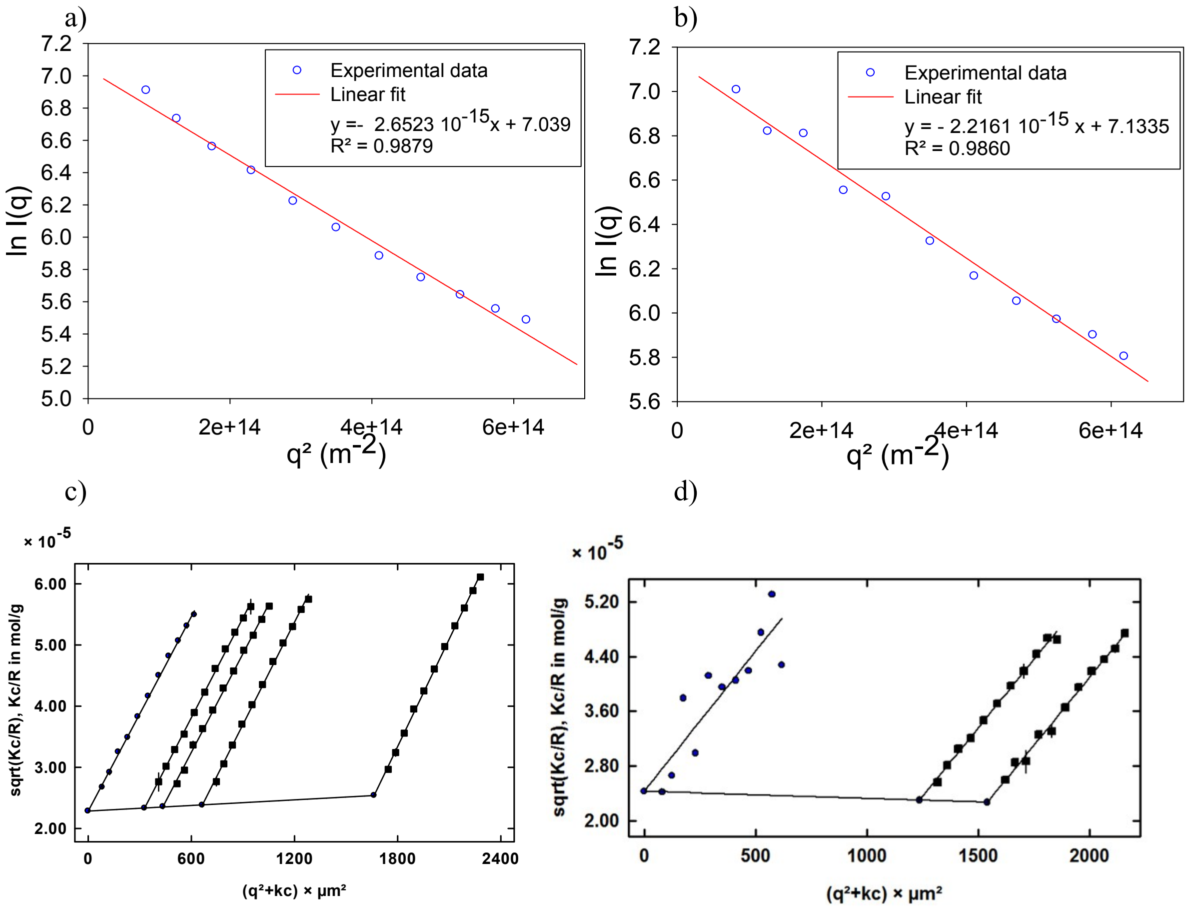

Figure S7. Multi-angle SLS plots: Guinier (a,b) and Berry (c,d) plots on nanoprecipitated objects made by co-assembly of PEO$_{45}$-*b*-PCL$_{111}$ with 7.6 nm USPIOs at 16% FWR (a,c) or with 4.2 nm USPIOs at 32% FWR (b,d). Scattering angles were varied from 40° to 140° and concentrations from 0.041mg·mL^{-1} (for 4.2 nm USPIO sample) to 0.554 mg·mL^{-1} (for 7.6 nm USPIO sample).

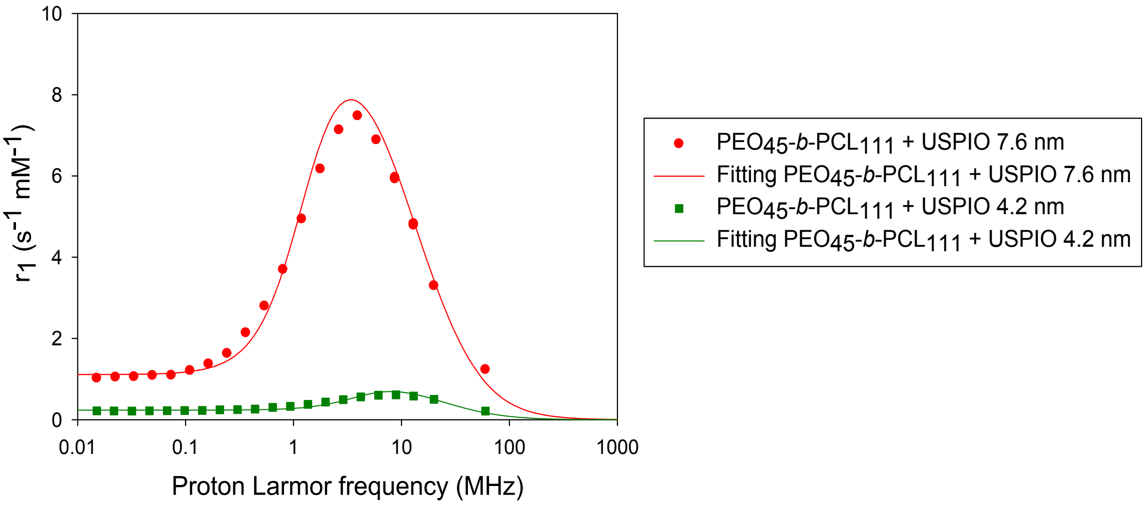

Figure S8. NMRD profiles of the longitudinal relaxivity *vs.* proton Larmor resonance frequency at 37°C for PEO_{45}-b-PCL_{111} vesicles loaded at 16% FWR with 7.6 nm USPIOs (circles) and at 32% FWR of 4.2 nm USPIOs (squares). The solid lines correspond to the MC simulation based on the theoretical model for superparamagnetic contrast agents.

Table S1. Parameters extracted from the fitted NMRD profiles (D^{NMRD} and M_S^{NMRD}) of USPIOs loaded in PEO_{45}-*b*-PCL_{111} vesicles (in water) and individually dispersed USPIOs (in THF).

Sample	D^{NMRD} (nm)	M_S^{NMRD} ($A{\cdot}m^2{\cdot}kg^{-1}$)
PEO_{45}-*b* -PCL_{111} vesicles + 7.6 nm USPIOs at 16% FWR (in water)	20.8	14.0
7.6 nm USPIO (in THF)	8.5	49.4
PEO_{45}-*b* -PCL_{111} vesicles + 4.2 nm USPIOs at 32% FWR (in water)	18.2	5.6
4.2 nm USPIO (in THF)	5.6	49.7

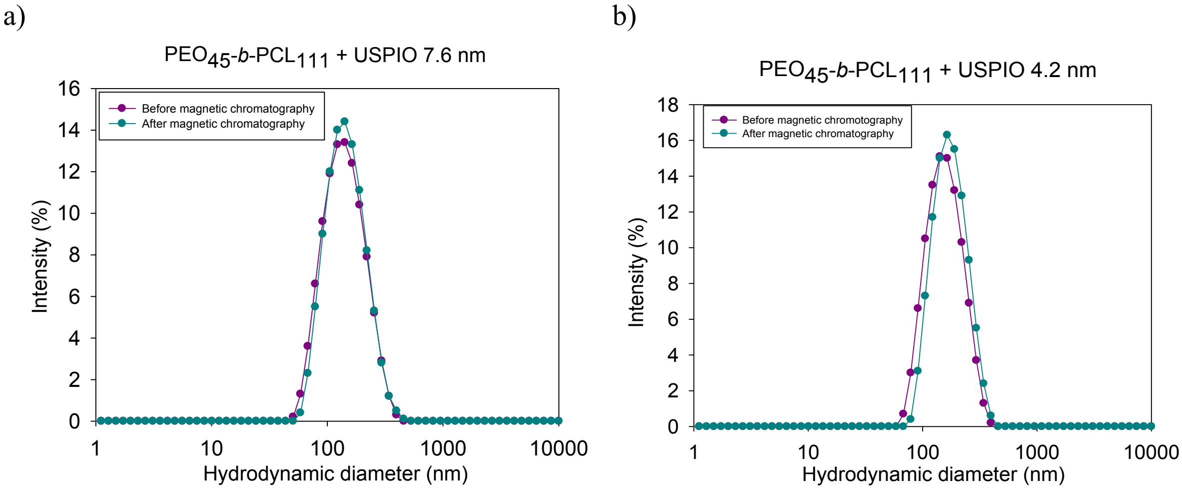

Figure S9. Intensity-weighted size distribution measured by DLS of PEO_{45}-*b*-PCL_{111} vesicles measured after synthesis and after magnetic chromatography (a) vesicles loaded at 16% FWR with USPIOs of 7.6 nm diameter and (b) vesicles loaded at 32% FWR with USPIOs of 4.2 nm diameter.

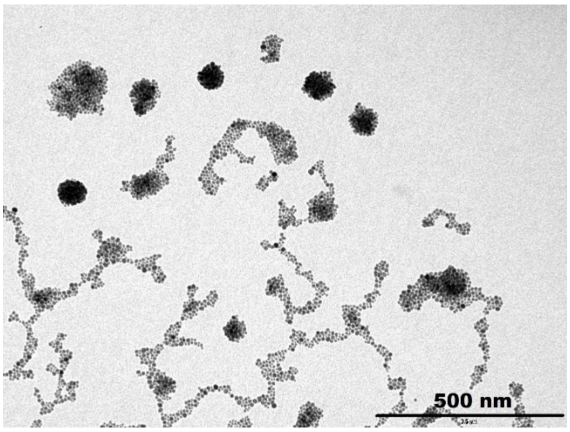

Figure S10. TEM image of PEO_{45}-*b*-PCL_{111} vesicles loaded at 16% FWR with iron oxide nanoparticles of 7.6 nm diameter after magnetic chromatography.

Table S2. Longitudinal (r_1) and transverse (r_2) relaxivities (in water and at 37°C) and resultant r_2/r_1 ratios of USPIO loaded in PEO_{45}-*b*-PCL_{111} vesicles before and after magnetic chromatography

Sample	Larmor frequency (MHz)	Before magnetic chromatography			After magnetic chromatography		
		r_1 ($s^{-1}\cdot mM^{-1}$)	r_2 ($s^{-1}\cdot mM^{-1}$)	r_2/r_1	r_1 ($s^{-1}\cdot mM^{-1}$)	r_2 ($s^{-1}\cdot mM^{-1}$)	r_2/r_1
PEO_{45}-*b*-PCL_{111} + USPIO 7.6 nm (FWR=16%)	20	3.23	187	58	2.85	172	60
	60	1.22	198	162	1.09	188	173
PEO_{45}-*b*-PCL_{111}+ USPIO 4.2 nm (FWR=32%)	20	0.64	109	171	0.55	94	171
	60	0.28	110	389	0.23	87	371

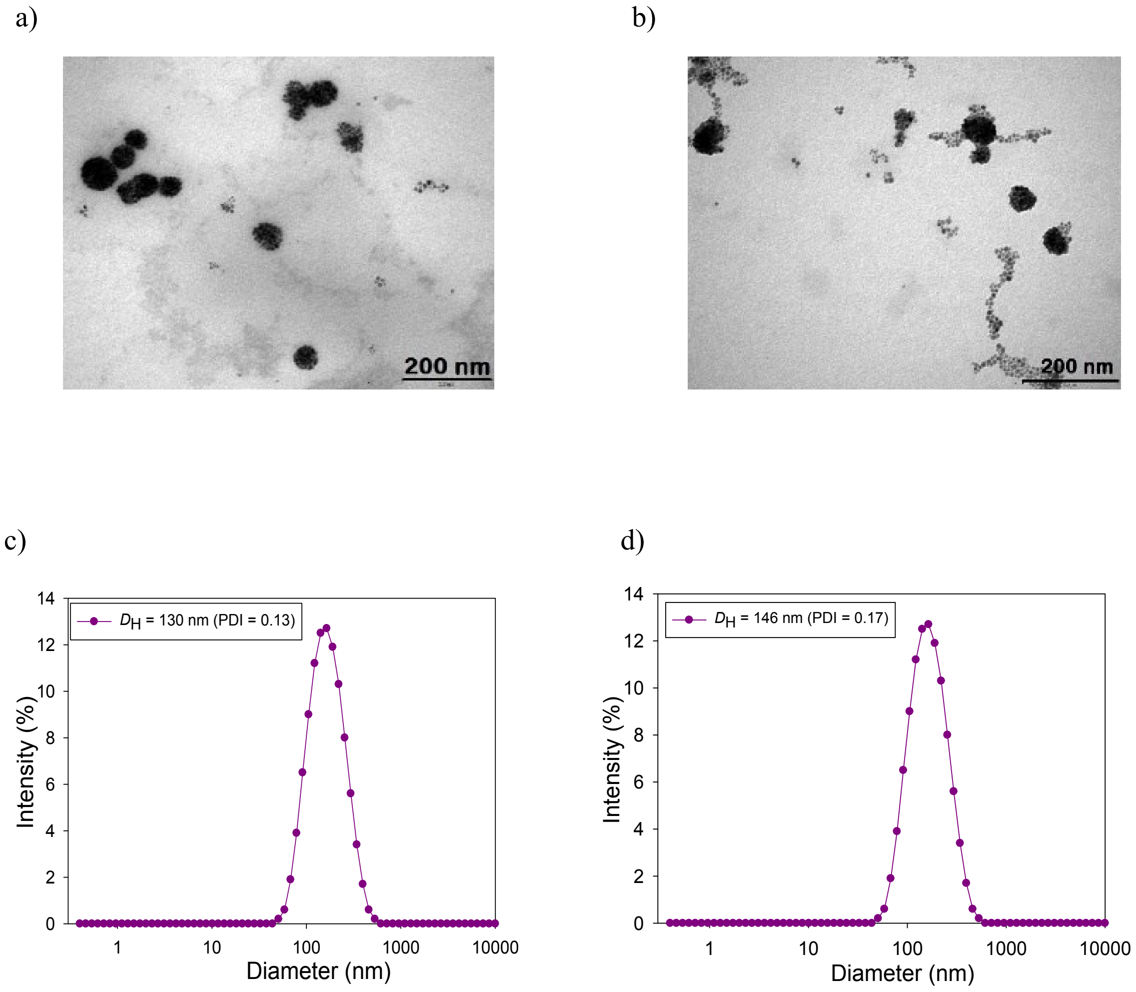

Figure S11. TEM images (a and b) and intensity-weighted size distributions (c and d) of PEO_{45}-*b*-PCL_{111} vesicles loaded at 16% FWR with 7.6 nm iron oxide nanoparticles: a) and c) sample left 7 days at 37°C and at pH 7 and b) and d) sample left 7 days at 37°C and at pH 5.

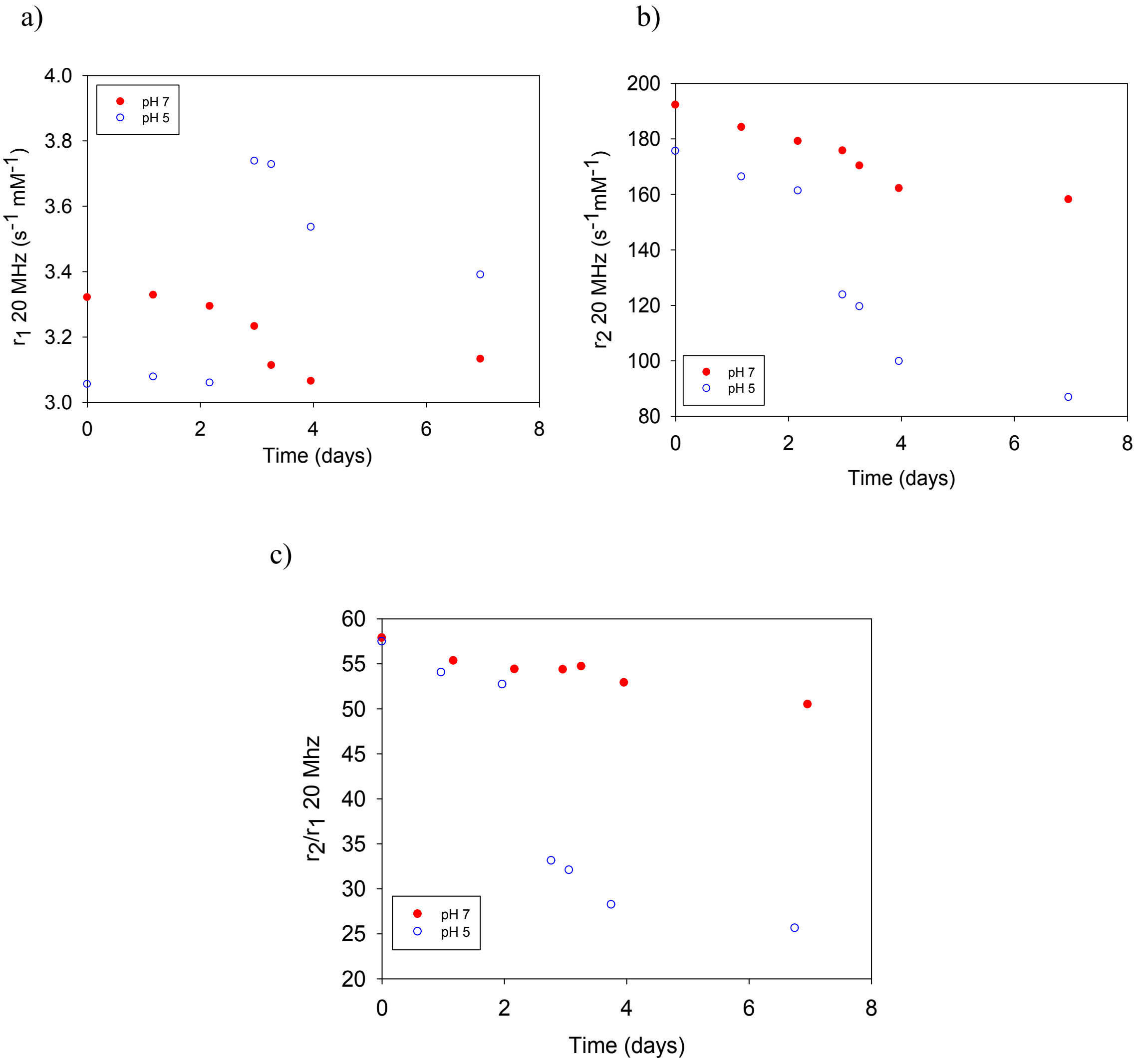

Figure S12. Longitudinal relaxivities (a), transverse relaxivities (b) and transverse to longitudinal relaxivity ratios (c) at 20 MHz for PEO$_{45}$-*b*-PCL$_{111}$ vesicles loaded at 16% FWR with 7.6 nm USPIOs at pH 7 (red markers) and pH 5 (blue markers) as function of time.